

1 Ultrametric diffusion equation on energy
2 landscape to model disease spread in
3 hierarchic socially clustered population

4 Andrei Khrennikov

Linnaeus University, International Center for Mathematical Modeling
in Physics and Cognitive Sciences Växjö, SE-351 95, Sweden

5 June 5, 2021

6 **Abstract**

7 We present a new mathematical model of disease spread reflect-
8 ing some specialties of the covid-19 epidemic by elevating the role of
9 hierarchic social clustering of population. The model can be used to
10 explain slower approaching herd immunity, e.g., in Sweden, than it was
11 predicted by a variety of other mathematical models and was expected
12 by epidemiologists; see graphs Fig. 1,2. The hierarchic structure
13 of social clusters is mathematically modeled with ultrametric spaces
14 having treelike geometry. To simplify mathematics, we consider trees
15 with the constant number $p > 1$ of branches leaving each vertex. Such
16 trees are endowed with an algebraic structure, these are p -adic number
17 fields. We apply theory of the p -adic diffusion equation to describe a
18 virus spread in hierarchically clustered population. This equation has
19 applications to statistical physics and microbiology for modeling *dy-*
20 *namics on energy landscapes*. To move from one social cluster (valley)
21 to another, a virus (its carrier) should cross a social barrier between
22 them. The magnitude of a barrier depends on the number of social
23 hierarchy's levels composing this barrier. We consider *linearly increas-*
24 *ing barriers*. A virus spreads rather easily inside a social cluster (say
25 working collective), but jumps to other clusters are constrained by
26 social barriers. This behavior matches with the covid-19 epidemic,
27 with its cluster spreading structure. Our model differs crucially from
28 the standard mathematical models of spread of disease, such as the
29 SIR-model; in particular, by notion of the probability to be infected
30 (at time t in a social cluster C). We present socio-medical specialties
31 of the covid-19 epidemic supporting our model.

32 **keywords:** energy landscapes; ultrametric spaces; p -adic num-
33 bers; ultrametric diffusion equation; social barriers; linear growing bar-
34 riers covid-19; epidemic; disease spread; herd immunity; hierarchy of
35 social clusters; superspreaders, asymptomatic individuals; rigid vs.
36 mild social restrictions.

37 1 Introduction

38 The covid-19 epidemic has many unusual features (see appendix 1).
39 One of them plays the crucial role in disease (say a virus) spread. We
40 formulate it as the basic assumption of this paper (see also [1]):

41 **ASO** *Virus' spread in population is constrained by the hierarchic*
42 *social cluster structure.*

43 How can one model mathematically hierarchic social clustering of
44 population? In a series of works [2]-[7], we constructed *ultrametric*
45 *clustering* of population by using the system of hierarchically ordered
46 social coordinates and this approach was applied in cognition, psychol-
47 ogy, sociology, information theory (see also [8]-[12]). In this paper, we
48 shall use ultrametric diffusion equation [13]-[21] to describe dynamics
49 of covid-19 spread in socially clustered population. It is important
50 to note that ultrametric spaces have treelike geometry and we study
51 virus' dynamics on social trees. To simplify mathematics, considera-
52 tion is restricted to homogeneous trees with p -branches leaving each
53 vertex. Such trees are endowed with an algebraic structure, these are
54 p -adic number fields \mathbf{Q}_p . We remark that p -adic numbers are widely
55 used in number theory and algebraic geometry. Their applications to
56 natural phenomena started with string theory and quantum physics
57 [22]-[24].

58 The specialties of covid-19 epidemic¹ are not reflected in the stan-
59 dard mathematical models [25]-[27], such as, e.g., the canonical SIR
60 model [28] and its diffusion-type generalizations, e.g., [29]. Conse-
61 quently, in spite of the tremendous efforts [30]-[36], mathematical
62 modeling of covid-19 spread cannot be considered as successful. There-
63 fore, we have to search for new mathematical models reflecting better
64 the covid-19 specialties. The recent paper [1] based on **ASO** can be
65 considered as a step in this direction. In it, we studied the problem of
66 *approaching herd immunity in heterogeneous socially clustered popula-*
67 *tion.* A virus does not spread throughout population homogeneously

¹See appendix 1, “covid on surface”, “covid in air”, “asymptomatic individuals”, “no mass-events”, “superspreaders”; in this paper we are interested in mild restrictions, as say in Sweden, i.e., without lock-down.

68 as it is described by the standard models of disease spread. Its spread
69 has the clear social cluster character (cf. with disease spread mod-
70 eling in articles [37]-[40], especially with the last paper as referring
71 to epidemic in Sweden). The virus spreads relatively easy in a social
72 cluster that was infected by somebody, but approaching other clusters
73 is constrained by social barriers.

74 Such virus spread is described very well by *dynamics on energy*
75 *landscapes*. The latter is well developed theory with numerous appli-
76 cations to statistical physics (e.g., spin glasses) and microbiology [41]-
77 [47]. An energy landscape is a system of (energy) valleys separated by
78 barriers of different heights having a hierarchic structure. A system
79 (physical, biological) can move inside a valley or jump over a barrier
80 to another valley, with some probability. Thus, the simplest math-
81 ematical model is given by *random walks on energy landscapes* (see,
82 e.g., [48]). Behavior of random walking depends crucially of grows of
83 barriers coupled to the hierarchic structure of an energy landscape.

84 Geometrically the hierarchy of valleys (clusters) of an energy land-
85 scape has the treelike structure. As is well known, trees also give
86 the geometric representation for ultrametric spaces and vice verse.
87 Thus, dynamics on energy landscapes, collection of clusters separated
88 by hierarchically ordered barriers, can be represented as dynamics in
89 ultrametric spaces.

90 In the first paper [1] on ultrametric approach to disease spread,
91 we explored the random walk in ultrametric spaces, see, e.g., [48] for
92 simple mathematical theory. Such random walk is the discrete version
93 of *ultrametric diffusion*. Theory of diffusion equations in ultrametric
94 space is well developed [13]-[21]. In the present paper, we apply its
95 powerful mathematical apparatus for modeling disease spread in hier-
96 archically structured social clusters. The problem of approaching herd
97 immunity is reformulated in terms of ultrametric diffusion equation.
98 This reformulation makes the model mathematically rigorous (studies
99 [41]-[47], [48] were at the physical level of rigorousness) and opens the
100 door for development of a variety of new mathematical models of dis-
101 ease spread taking into account the hierarchic social cluster structure
102 of population.

103 We consider a country relatively mild preventing measures² and
104 model this situation with linearly increasing barriers; context of rigid
105 preventing measures as say lock-down can be modeled with exponen-
106 tially increasing barriers.

107 For Sweden, this problem of approaching herd immunity is of the
108 big value. The country did not impose the lock-down and the system

²See [1], appendix 2 for compact description of situation in Sweden, March-June 2020, from the viewpoint of imposing social barriers.

109 of measures presented by the state epidemiologist Anders Tegnell and
 110 his team was aimed to approach herd immunity and, in this way, to
 111 make essentially weaker or escape at all the second wave of covid-
 112 19 epidemic and may be proceed without vaccination. However, the
 113 dynamics of population's immunity against coronavirus is very slow,
 114 essentially slower than it was predicted by Swedish epidemiologists
 115 and by mathematical models of disease spread ³ (see, e.g., [49]-[51] for
 116 reports from Public Health Institute of Sweden, [32]-[34] for attempts
 117 of mathematical modeling and [52]-[56] for reports from massmedia).

118 As we have seen [1], ultrametric random walk (with jumps over
 119 mild barriers linearly growing with levels of social hierarchy) generates
 120 dynamics with asymptotic behavior of the power type; herd immunity
 121 in a social cluster C grows as

$$p_{\text{Im}}(C, t) = 1 - t^{-q}, q > 0. \quad (1)$$

122 Generally (but, of course, depending on the parameter q) this function
 123 increases slowly. This asymptotic can explain unexpectedly slow ap-
 124 proaching herd immunity during covid-19 epidemic, say in population
 125 of Sweden. The basic parameter of the model

$$q = T \ln p / \Delta. \quad (2)$$

126 Here $T > 0$ is the social analog of temperature, the degree of activity in
 127 a society, Δ is the magnitude of the elementary barrier for hopping be-
 128 tween nearest social levels. Higher social temperature T implies more
 129 rapid approaching of herd immunity; higher social barrier Δ implies
 130 slower growth of herd immunity. Quantity $\ln p$ can be interpreted as
 131 entropy of virus spreading inside a social cluster, $\mathcal{E} = \ln p$, (see (??)).
 132 This entropic interpretation leads to conjecture that more general pro-
 133 cesses of disease spread (with the same linear growth of barriers) would
 134 lead to the following asymptotics for approaching herd immunity:

$$p_{\text{Im}}(C, t) = 1 - t^{-\frac{T\mathcal{E}}{\Delta}}. \quad (3)$$

135 In the present paper, by using results of work [17] on the relax-
 136 ation dynamics for diffusion pseudo-differential equation on ultramet-
 137 ric spaces we reproduce the power law for dynamics of herd immunity
 138 [1], for linearly growing barriers. The technique of ultrametric diffu-
 139 sion equations provides the possibility to study this problem for other

³In particular, by models Tom Britton [32, 33] that was used by Swedish State Health Authority predicted that herd immunity will be approached already in May; Anders Tegnell also announced, starting from the end of April 2020, that Sweden would soon approach herd immunity, but it did not happen, neither in May, nor June and July.

140 types of barriers as well as for design of more general mathematical
141 models of disease spread.

142 Just before submission of preprint [1], I found the recent paper
143 of Britton et al. [40] in that the role of population heterogeneity in
144 spread of covid-19 was analyzed. We remark that Britton contributed
145 a lot in mathematical modeling of covid-19 spread in Sweden. His
146 models [32, 34] were explored by chief epidemiologist Anders Tegnell
147 to justify the Swedish policy with respect to epidemic - no lock-down as
148 expecting rapid approaching herd immunity. On the basis of Britton’s
149 models, Swedish State Health Authority predicted (at the end of April
150 2020) that the herd immunity will be approached already in May.
151 However, this prognoses did not match the real situation and the herd
152 immunity was not approached neither in May nor in June (see, e.g.,
153 [49]-[51] for reports from Public Health Institute of Sweden, see also
154 [52]-[56]). In previous modeling [32, 34] for covid-19 epidemic, Swedish
155 population was considered as homogeneous. In [40], heterogeneity of
156 population was considered as an important factor; the model involves
157 two “social coordinates” (in our terminology): *social activity and age*.

158 Taking into account population social clustering is the basic simi-
159 larity of our models (see also appendix 3) and generally paper [40]
160 is supporting for our approach. The main difference is that in [40]
161 the hierarchic structure of social clustering and hence the hierarchy
162 of barriers between clusters is not taken into account. Another cru-
163 cial difference is in mathematical methods, based on the real metric
164 vs. ultrametric. Surprisingly, these two totally different mathematical
165 models led to graphs of the same shape, see Fig. 2 and see Fig. S2,
166 supplementary material [40]. Both models provide the possibility to
167 play with strength of preventive measures and see their effect onto the
168 epidemics’ dynamics.

169 2 Hierarchic treelike geometry of so- 170 cial clusters

171 We represent the human society as a system of hierarchically cou-
172 pled (as a treelike structure) disjoint clusters. There are many ways
173 for mathematical modeling of such representations. Theory of *ultra-*
174 *metric spaces* is one of the basic mathematical tools for this purpose.
175 Geometrically ultrametric spaces can be represented as trees with hier-
176 archic levels. Ultrametricity means that this metric satisfies so-called
177 strong triangle inequality:

$$\rho(x, y) \leq \max\{\rho(x, y), \rho(y, z)\}, \quad (4)$$

178 for any triple of points x, y, z . Here in each triangle the third side is
179 less or equal not only the sum of two other sides (as usual), but even
180 their maximum. Define balls as usual in metric spaces $B_R(a) = \{x : \rho_p(x, a) \leq R\}$, where a is a center of the ball and $R > 0$, is its radius.
181 The balls have the following basic properties:
182

- 183 • Two balls are either disjoint or one of them is contained in an-
184 other.
- 185 • Any point of a ball can be selected as its center, i.e., $B_R(a) =$
186 $B_R(b)$ for any $b \in B_R(a)$.

187 Any ball can be represented as disjoint union of balls of smaller
188 radius, each of the latter can be represented in the same way with even
189 smaller radius and so on. We get hierarchy of balls corresponding to
190 disjoint partitions. Geometrically a ball is a bunch of branches of a
191 tree.

192 We use the ultrametric balls to represent mathematically social
193 clusters, any cluster is slit into disjoint sub-cluster, each of the latter
194 is split into its own (disjoint) sub-clusters and so on. Inclusion relation
195 generates the hierarchy on the set of social clusters.

196 In a series of works of the author and his collaborators [2]-[6], ultra-
197 metric spaces (geometrically hierarchic trees) were applied for model-
198 ing of cognitive, psychological, and social phenomena. This modeling
199 was based on invention of systems of discrete social (or mental in
200 cognitive studies) coordinates $x = (x_m)$ characterizing (psycho-)social
201 states of individuals. The treelike representation of *social states* is
202 based on selection of hierarchically ordered social factors enumerated
203 by index $m \in \mathbf{Z} = \{0, \pm 1, \pm 2, \dots\}$. (It is convenient to work with co-
204 ordinates enumerated by integer numbers.) The social importance of
205 coordinates x_m decreases with increase of m and increases with de-
206 crease of m ; e.g., social coordinate x_0 is more important than any
207 $x_j, j > 0$, but it less important than any $x_j, j < 0$. The coordinate
208 x_0 can be considered as a reference point. Depending on context (say
209 socio-economic or socio-epidemic) it can be shifted to the right or
210 to the left. Therefore it is convenient to use positive and negative
211 indexes determining two different directions of social importance of
212 coordinates.

213 We consider discrete social coordinates, generally, for each m , there
214 N_m possible values, $x_m = 0, 1, \dots, N_m - 1$, and N_m can vary essentially
215 with m . In the treelike representation, numbers N_m determine the
216 number of branches leaving vertexes. Such trees are complicated and
217 we restrict modeling to homogeneous trees for that N_m does not dep-
218 end on m . Moreover, by pure mathematical reasons it is convenient
219 to select $N_m = p$, where $p > 1$ is the fixed prime number. We remark

220 that the corresponding theory was developed even for arbitrary trees
221 (ultrametric spaces), but it is essentially more complicated [18, 19].

222 Thus, a social state x is represented by a vector of the form:

$$x = (x_{-n}, \dots, x_{-1}, x_0, x_1, \dots, x_m), \quad x_j \in \{0, 1, \dots, p-1\}. \quad (5)$$

223 The vector representation of psychical, mental, and social states is very
224 common in psychology and sociology. The essence of our approach [2]-
225 [6] is the hierarchic ordering of coordinates leading to introduction of
226 ultrametric on the state space, see (8).

227 For our purpose, modeling of epidemic, we can consider, for exam-
228 ple, the following hierarchic system of social coordinates; for simplicity,
229 let index $m = 0, 1, 2, \dots$, so the coordinate x_0 is the most important.
230 It is natural to use it to denote states (e.g., Sweden, Russia, USA,...);
231 x_1 can be used for age; x_2 for chronic diseases, x_3 gender, x_4 for race,
232 x_5 for the town of location, x_6 for the district, x_7 for profession, x_8 for
233 the level of social activity, x_9 for the number of children, and so on.
234 We understand that such ranking of the basic social factors related to
235 the covid-19 epidemic is incomplete. The contribution of sociologists,
236 psychologists, and epidemiologists can improve the present model es-
237 sentially, see even the recent article [57] on mathematical model of
238 evolutionary creation of social types and contribution of genetics and
239 natural selection.

240 Since the majority of states selected the lock-down policy that was
241 not oriented towards approaching herd immunity, we restrict consid-
242 eration to the Swedish population. So, in the above assigning of social
243 meaning to coordinates they are shifted to the left. We also stress that
244 hierarchy of social factors involved in the covid-19 epidemic can be se-
245 lected depending on the state, i.e., for each state we create its own
246 system of social clustering coupled to this epidemic. Consider USA,
247 here the population is not so homogeneous with respect to the level
248 of income and the life style connected to income as it is in Sweden.
249 The social factor of belonging to up or low income classes plays the
250 crucial role in covid-19 infecting. It seems that this coordinate should
251 be places as the next (to the right) to the age-coordinate, then the
252 race-coordinate and so on. Thus, the above hierarchy, (age, chronic
253 disease, gender, race, town, district, family,...), that is appropriate
254 for Sweden, should be rearranged for USA, as say (age, income, race,
255 chronic disease, gender, town, district, family,...).⁴

256 It is convenient to proceed with variable number of coordinates,
257 i.e., not fix n and m . This gives the possibility to add new coordinates.
258 The space of such vectors can be represented by rational numbers of

⁴Income did not play any role in Sweden during the covid-19 epidemic.

259

the form

$$x = x_{-n}p^{-n} + \dots + x_{-1}p^{-1} + x_0 + x_1p + \dots + x_m p^m, \quad x_j \in \{0, 1, \dots, p-1\}. \quad (6)$$

260

This is the basis of the number-theoretic representation of the space of social states. We shall consider it later. Now we continue in the vector framework.

261

262

263

To use fruitfully ultrametric models, we have to construct a complete metric space. The standard way to achieve completeness is to consider infinite sequences of the form:

264

265

$$x = (\dots, x_{-n}, \dots, x_{-1}, x_0, x_1, \dots, x_m, \dots), \quad x_j \in \{0, 1, \dots, p-1\}, \quad (7)$$

266

where, for each x , there exists n such that $x_{-j} = 0, j > n$. Denote the space of such sequences by the symbol \mathbf{Q}_p . On this space, a metric is introduced in the following way. Consider two sequences $x = (x_j)$ and $y = (y_j)$; let $x_j = y_j, j < n$, where n is some integer, but $x_n \neq y_n$. Then the distance between two vectors is defined as

267

268

269

270

$$\rho_p(x, y) = p^{-n}. \quad (8)$$

271

So, if n is negative, then distance is larger than 1, if n is nonnegative, then distance is less or equal to 1. The ρ_p is an ultrametric. We remark that each ball can be identified with a ball of radius $R = p^n, n \in \mathbf{Z}$. Ball $B_1(0)$ plays the important role and it is defined by special symbol \mathbf{Z}_p . As in any ultrametric space, each ball is represented as disjoint union of smaller balls, e.g.,

272

273

274

275

276

$$\mathbf{Z}_p = \cup_{j=0}^{p-1} B_{1/p}(a^j) = \cup_{j_0 \dots j_{n-1}=0}^{p-1} B_{1/p^n}(a^{j_0 \dots j_{n-1}}) \quad (9)$$

277

where $a^j \in \mathbf{Z}_p$ is constrained by condition $x_0 = j$ and $a^{j_0 \dots j_{n-1}}$ is constrained by conditions $x_0 = j_0, \dots, x_{n-1} = j_{n-1}$, and so on. We recall that in an *ultrametric space*, any point of a ball can be selected as its center.

278

279

280

281

In our model, p -adic balls represent social clusters corresponding to fixing a few social coordinates. For example $C_j = B_{1/p}(a^j) = \{x \in \mathbf{Z}_p : x_0 = j\}$, in above epidemic coding C_j corresponds to fixing age= j ; $C_{ji} = B_{1/p}(a^{ji}) = \{x \in \mathbf{Z}_p : x_0 = j, x_1 = i\}$, age= j , gender= i for Swedish society or age= j , income level= i for American society.

282

283

284

285

286

Social states, points of \mathbf{Q}_p , can be considered as balls of zero radius, we call them *elementary social clusters*. Partitions of a ball into disjoint balls of smaller radii corresponds to partition of a social cluster into disjoint subclusters of deeper level of social hierarchy.

287

288

289

290

Now we turn to the algebraic representation of social states by rational numbers, see (6). The space \mathbf{Q}_p endowed with ultrametric ρ_p

291

292 can be considered as completion of this set of rational numbers and
 293 algebraically the elements of \mathbf{Q}_p can be represented by power series of
 294 the form

$$x = \sum_{k=n} x_k p^k \quad (10)$$

295 where $x_j \in \{0, 1, \dots, p-1\}$, $x_n \neq 0$, and $n \in \mathbf{Z}$; so only finite number
 296 of coordinates with negative index k can differ from zero. Such a se-
 297 ries converges with respect to ultrametric ρ_p . Representation by the
 298 power series gives the possibility to endow \mathbf{Q}_p with the algebraic opera-
 299 tions, addition, subtraction, multiplication, and division (the latter
 300 operation is defined only for prime p). Hence, \mathbf{Q}_p is a *number field*,
 301 *the field of p -adic numbers*. This algebraic representation leads to
 302 number-theoretic representation of ultrametric, $\rho_p(x, y) = |x - y|_p$,
 303 where $x \rightarrow |x|_p$ is the p -adic analog of the real absolute value; per
 304 definition, for x given by series (10),

$$|x|_p = \left| \sum_{k=n} x_k p^k \right|_p = p^{-n}. \quad (11)$$

305 It satisfies the strong triangle inequality playing the fundamental role
 306 in p -adic analysis and implying (4):

$$|x + y|_p \leq \max\{|x|_p, |y|_p\}. \quad (12)$$

307 **3 Probability to become infected as** 308 **contextual probability**

309 The quantity $p_I(C, t)$, the probability that a person belonging to social
 310 cluster C can become infected at the instant of time t , is the basic
 311 quantity of our model. Therefore, it is useful to discuss its meaning
 312 in more detail.

313 First of all, we point to the difference from the standard SIR-like
 314 models: $p_I(C, t)$ is not the proportion of infected people in cluster C
 315 at the instant of time t , i.e.,

$$p_I(C, t) \neq \frac{N_I(C, t)}{N}, \quad (13)$$

316 where N is the number of people in C and $N_I(C, t)$ is the number of
 317 infected people in C at the instant of time t . Thus, $p_I(C, t)$ has no
 318 straightforward relation to the number of infected people $N_I(C, t)$. Of
 319 course, $p_I(C, t)$ depends on $N_I(C, t)$, but not simply as frequency (13).

320 Probability $p_I(C, t)$ is determined by context $\mathcal{C}(C, t)$, the complex
 321 of social, economic, and epidemiological conditions in cluster C at the

322 instant of time t , i.e., this is *contextual probability*. Such probabilities
323 are considered, e.g., in quantum theory [58], where it is difficult, if
324 possible at all, to introduce “hidden variables” determining probabil-
325 ities. We remark that the situation in epidemiology, especially with
326 respect to the covid-19 epidemic, is similar to quantum physics and
327 more general quantum-like modeling in cognition, psychology, and de-
328 cision making [59, 60]. It is impossible to determine “hidden variables”
329 behind many events (see appendix 3). So, people and social clusters
330 of people definitely reacts to covid-19 in very different ways, there are
331 bio-medical, social, and may be even psychological hidden variables.
332 Context $\mathcal{C}(C, t)$ determines their distribution, but it seems to be im-
333 possible to find these probability distributions and their dependence
334 on contexts.

335 One of the possibilities to interpret the probability to become in-
336 fected in context $\mathcal{C}(C, t)$ is to use the subjective interpretation of prob-
337 ability.⁵ By this interpretation $p_I(C, t)$ is subjective probability that
338 is assigned by an individual to the event that by visiting social clus-
339 ter C one would become infected (she is an arbitrary individual, she
340 need not belong to social cluster C). We stress that a social cluster
341 is a domain in social space, so it need not be determined simply by
342 geography (although geographic location place the important role in
343 determination of C). Subjective probability is widely used in decision
344 making as a part of subjective utility theory. During some epidemic,
345 people can be considered as decision makers who should estimate the
346 probability to become infected by eating lunch with colleagues or din-
347 ner with friends, going to shopping mall, visiting Stockholm - for me,
348 it was everyday decision problem during March-June 2020, and I re-
349 ally estimated the probability to become infected by covid-19; for my
350 American friend from New York, similar decisions were about to go
351 to Bronx or Manhattan, to barber (in June 2020) and so on. So, the
352 subjective probability approach, although not so common in epidemi-
353 ology, seems to be really natural for individuals’ everyday decision
354 making.

355 The problem under consideration is by knowing probabilities to
356 become infected in social clusters $C_i, i = 1, \dots, M$, at time t_0 , $p_I(C_i, t_0)$,
357 to estimate the probability for cluster C_k at later instances of time
358 $t > t_0$, $p_I(C_k, t)$. Dynamics $t \rightarrow p_I(C_k, t)$ is described by the *master*
359 *equation*. To write this equation, we have to consider conditional
360 probabilities (also known as transition probabilities): $p(C_k|C_i; t)$ is
361 the probability, for a person in social cluster C_k , to get infection from
362 a person from cluster C_i . These conditional probabilities represent

⁵We remark that this interpretation became popular even in quantum physics, under the name of Quantum Bayesianism (QBism) [61].

363

intensities to become infected. The master equation has the form:

$$\frac{d}{dt}p_I(C_k, t) = \sum_{i \neq k} [p(C_k|C_i; t)p_I(C_i, t) - p(C_i|C_k; t)p_I(C_k, t)]. \quad (14)$$

364

By using infinitesimals, we can write this probability balance equation in the form:

365

$$p_I(C_k, t+dt) = p_I(C_k) + \sum_{i \neq k} [p(C_k|C_i; t)p_I(C_i, t) - p(C_i|C_k; t)p_I(C_k, t)]dt. \quad (15)$$

366

367

368

369

370

371

372

373

374

375

376

377

378

379

380

381

382

383

384

385

386

The term $p(C_k|C_i; t)p_I(C_i, t)$ gives the intensity of transition of infection from cluster C_i to cluster C_k . Thus the probability to become infected in cluster C_k increases due to transfer of infection from other clusters. Thus meaning of the positive term in the right-hand side of (15) is clear. Negative term describes the “flow of infection” from C_k to other clusters. This flow generates decrease of the probability to become infected in C_k . To describe the latter process, we should consider disease spreaders and their transitions between social clusters, say from Bronx to Manhattan and vice versa. The quantity $p(C_k|C_i; t)p_I(C_i, t)$ gives the probability that somebody from social cluster C_k (Manhattan) would be infected by somebody who comes to C_k from C_j (say from Bronx). But at the same time some infected people from Manhattan, C_k can go to Bronx, C_i , and infect people here. By being busy with infecting people in Bronx, people from Manhattan cannot infect people in their own social cluster, so the probability to become infected in Manhattan decreases by $p(C_i|C_k; t)p_I(C_k, t)dt$.

Latter, in section 5, we shall consider the random walk model of virus spreaders. As was pointed out, the main distinguishing feature of this model is the hierarchic social clustering of population and the presence of barriers between clusters. Barrier’s height depends of the (social) distance between clusters.

387

388

389

390

391

392

393

394

395

396

397

398

399

Finally, we present the mechanical model for the above process of infection flow between social clusters. We can consider clusters as virus reservoirs, $p_I(C, t)$ gives the virus concentration in cluster C at time t . Once again, the presence of barriers increasing with hierarchy levels plays the crucial role in dynamics of virus’spread in population.

This probability is interpreted as in statistical mechanics of gases: as the concentration of virions (virus particles, consisting of nucleic acid surrounded by a protective coat of protein called a capsid) in cluster C that is interpreted as reservoir of virions. Now, we identify probabilities, $P(C, t) = P_I(C, t)$: probability to become infected is determined by concentration of virions in this cluster. Of course, concentration of virions is coupled with concentration of infected people, but not straightforwardly, since

400

- virions can live on various surfaces;

401

- covid-19 epidemic demonstrated the crucial role of superspreaders - super-powerful sources covid-19 virions [66] (see appendix 2).

402

403

404

Then $p(C_k|C_i;t)$ describes the intensity of transition of virions from cluster C_i to cluster C_k .

405

406

4 Modeling the virus spread with ultrametric diffusion equation

407

408

An elementary social cluster (social state) given by a point of \mathbf{Q}_p is a mathematical abstraction. Real clusters are represented by balls of finite radii. Therefore it is interesting to study the evolution of average probability for cluster $C \equiv B_{p^n}(0), n = 0, \pm 1, \pm 2, \dots$. Under assumption **AS3**, this quantity is represented as the integral with respect to the Haar measure:

409

410

411

412

413

$$p_I(C, t) = \int_C p_I(x, t) \mu(dx). \quad (16)$$

414

Under the above assumptions on the social structure of population and its interaction with the virus (including restrictions imposed by authorities in connection with epidemic), we can write the following master equation for probability $p_I(x, t)$,

415

416

417

$$\frac{\partial p_I(x, t)}{\partial t} = \int_{Q_p} [p(x|y; t)p_I(y, t) - p(y|x; t)p_I(x, t)] \mu(dy), \quad (17)$$

418

where $p(x|y; t)$ is the transition probability: the probability that the virus being present in (elementary) cluster y would jump to cluster x . We suppose that this probability does not depend on time t and it is symmetric, i.e., $p(x|y) = p(y|x)$. Under these assumptions, the master equation has the form

419

420

421

422

$$\frac{\partial p_I(x, t)}{\partial t} = \int_{Q_p} p(x|y)[p_I(y, t) - p_I(x, t)] \mu(dy). \quad (18)$$

423

It is natural to assume that the transition probability decreases with increasing of the distance between two clusters, for example, that

424

$$p(x|y) = \frac{C_\alpha}{|x - y|_p^{1+\alpha}}, \quad \alpha > 0. \quad (19)$$

425

Here $C_\alpha > 0$ is a normalization constant, by mathematical reasons it is useful to select distance's power larger than one. This function

426

427 rather slowly approaches zero if the distance between points goes to
428 infinity. Thus, *the probability of transmission of infection from cluster*
429 *y to cluster x for socially distant clusters is practically zero.* This is
430 an important property of the model. In fact, it implies slower (than in
431 the standard models of disease spread) approaching herd immunity:
432 for a virus, it difficult to spread between socially distant clusters. We
433 also remark that if the distance between points goes to zero, then the
434 probability (in fact, its density) approaches infinity. *This implies very*
435 *rapid spread of infection in small social clusters.* In contrast to the
436 standard SIR-like models, in our model the probability of transmission
437 of infection depends crucially on social distance.

438 Hence,

$$\frac{\partial p_I(x, t)}{\partial t} = C_\alpha \int_{Q_p} \frac{p_I(y, t) - p_I(x, t)}{|x - y|_p^{1+\alpha}} \mu(dy). \quad (20)$$

439 The integral operator in the right-hand side is the operator of frac-
440 tional derivative D^α (the Vladimirov operator), see [13]. Thus, the
441 dynamics of the probability to become infected for those belonging
442 to an elementary social cluster is described by *the p-adic diffusion*
443 *equation:*

$$\frac{\partial p_I(x, t)}{\partial t} = D^\alpha p_I(x, t). \quad (21)$$

To formulate the Cauchy problem, we have to add some initial prob-
ability distribution. We select the uniform probability distribution
concentrated on a single ball, initially infected social cluster C ,

$$p_I(x, 0) = \frac{1}{\mu(C)} \begin{cases} 1, & x \in C \\ 0, & x \notin C \end{cases}$$

444 This equation and its various generalizations were studied by many
445 authors, for applications to physics and biology and by pure mathe-
446 matical reasons, see, e.g., [13]. We are interested in the relaxation
447 regime, i.e., asymptotic of average probability $p_I(C, t)$ for large t . We
448 use the mathematical result from [17] (see also [18, 19]) and obtain
449 that the average probability has the power behavior:

$$p_I(C, t) \sim t^{-1/\alpha}, \quad t \rightarrow \infty. \quad (22)$$

450 Thus the average probability to become infected in a social cluster
451 decreases rather slowly with time. If parameter α is relatively large
452 i.e., the virus transition probability decreases very quickly with in-
453 crease of the distance between social clusters, then $p_I(C, t)$ decreases
454 very slowly with time, it is practically constant (see the upper graph
455 at Fig. 1). If parameter α is relatively small, so the virus transi-
456 tion probability decreases slowly with increase of the distance, then

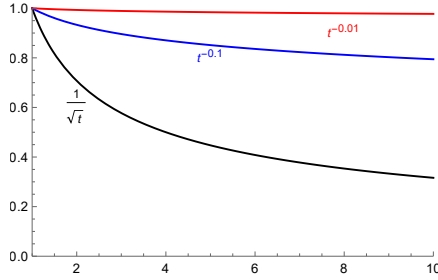


Figure 1: Asymptotic behavior of probability to become infected, transition probability parameter $\alpha = 2, 10, 100$.

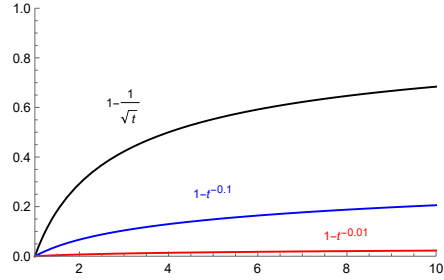


Figure 2: Asymptotic behavior of probability to become immune, transition probability parameter $\alpha = 2, 10, 100$.

457 $p_I(C, t)$ decreases sufficiently quickly with time (see the lowest graph
 458 at Fig. 1). We shall discuss these behaviors in section 5 by assigning
 459 bio-social meaning to the parameter α and by coupling it with the
 460 degree of preventing measures established by authorities. We present
 461 some graphs corresponding to different values of α at Fig. 1.

462 Consider now a kind of “integral immunity”, combination of innate
 463 and adaptive components, defined as the probability of not become
 464 infected:

$$p_{\text{Im}}(x, t) = 1 - p_I(x, t) \quad (23)$$

465 and its average over social cluster represented by ball C ,

$$p_{\text{Im}}(C, t) = 1 - p_I(C, t) \quad (24)$$

466 This function increases relatively slowly with time, see Fig. 2. Its
 467 asymptotic behavior depends on the parameter α determining how
 468 rapidly the transition probability between social clusters decreases
 469 with increase of the distance between them. The lowest graph cor-
 470 responds to large value of α , i.e., infection transition probability de-
 471 creases very quickly. Then $p_{\text{Im}}(C, t)$ is practically constant, herd im-
 472 munity increases very slow.

473 Parameter α combines two different factors:

- 474 • Traditional social constraints in population.
- 475 • Preventing measures imposed by state authorities.

476 It is clear that existing of traditional rigid social barriers in popu-
 477 lation has similar effect as imposing of rigid preventing measures by

478 authorities. The parameter α can be represented as sum of two com-
 479 ponents, $\alpha = \alpha_{\text{soc}} + \alpha_{\text{preventing}}$. For two populations (say countries)
 480 with large and small traditional social barriers α_{soc} , respectively, the
 481 same dynamics of herd immunity can be approached with small and
 482 large preventing barriers $\alpha_{\text{preventing}}$, respectively. Say in Japan α_{soc} is
 483 relatively large and in Italy it is relatively small, so mild preventing
 484 measures in Japan would correspond to rigid preventing measures in
 485 Italy.

486 However, this decomposition of α into two factors makes the model
 487 too complicated. It is better to restrict it to one concrete country; here
 488 α_{soc} is fixed and one can play with parameter $\alpha_{\text{preventing}}$ to compare
 489 different scenarios.

490 5 Virus' random walk on the hierar- 491 chic social tree

492 The mathematical result on the relaxation regime for the p -adic diffu-
 493 sion [17] is generalization of studies on random walks on ultrametric
 494 spaces describing dynamics on energy landscapes [48]-[47]. There are
 495 given energy barriers Δ_m separating valleys, movement from one val-
 496 ley to another valley is constrained by necessity to jump over a barrier
 497 between them. This random walk model gives a good heuristic pic-
 498 ture of the virus spread, as jumping from one social cluster (valley)
 499 to another, where clusters (valleys) are separated by social barriers
 500 (mountains) of different heights. Geometrically such random walk is
 501 represented as jumps on a tree between the levels of social hierarchy.
 502 Our model (selection of the transition probability in the form (19))
 503 corresponds to *barriers growing linearly with the number of elemen-*
 504 *tary jumps*. The relaxation regime of the power form is obtained for
 505 the number of hierarchy's levels approaching infinity, i.e., for ideal
 506 trees with infinitely long branches, as ultrametric spaces they are rep-
 507 resented by \mathbf{Q}_p .

508 The virus plays the role of a system moving through barriers in
 509 models of dynamics on energy landscapes (see [48], [41]-[47] and ref-
 510 erences herein). In our case, these are social barriers between social
 511 clusters of population. The virus performs a complex random walk
 512 motion inside each social cluster moving in its sub-clusters, goes out
 513 of it and spreads through the whole population, sometimes the virus
 514 comes back to the original cluster from other social clusters that have
 515 been infected from this initial source of infection, and so on. During
 516 this motion the virus should cross numerous social barriers.

517 Instead of virus walking through the social tree, we can consider

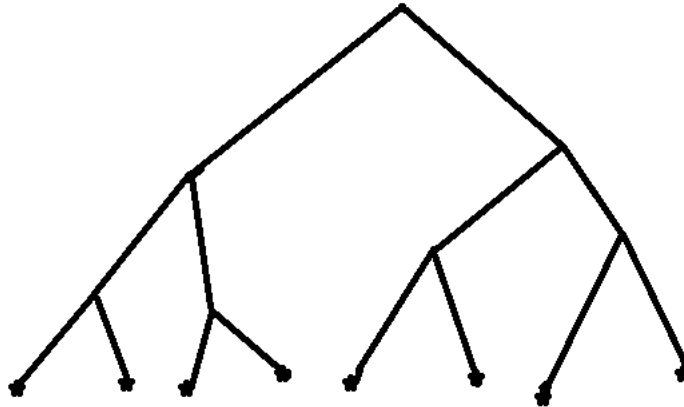


Figure 3: Treelike configuration space

518 a person. A person of the social type x can interact with persons of
 519 other social types. The temporal sequence of social contacts of some
 520 persons can have a very complicated trajectory, visiting numerous
 521 clusters (but the probability of approaching a cluster depends crucially
 522 on social barriers).

523 Let virus encounters a barrier of size Δ_m , in hopping a distance m
 524 (crossing m levels of hierarchy), where $\Delta_1 < \Delta_2 < \dots < \Delta_m < \dots$. It
 525 is supposed that barriers Δ_m are the same for all social clusters, i.e.,
 526 they depend only on distance, but not on clusters. This assumption
 527 reflects a kind of epidemic *égalité* of all social groups, the barriers
 528 preventing spread of the virus that are imposed by state authorities
 529 are the same for all social groups.

530 Consider the tree at Fig. 3. We identify the lengths of branches
 531 between vertexes with magnitudes of barriers. Then the barriers on
 532 this tree depend on clusters, so from this viewpoint the social tree is
 533 not homogeneous.

534 Consider the energy landscape with a uniform barrier Δ , at every
 535 branch point; that is, a jump of distance 1 involves surmounting a
 536 barrier Δ , of distance 2, a barrier 2Δ , and so on. Hence, barriers
 537 linearly grow with distance m ,

$$\Delta_m = m\Delta, m = 1, 2, \dots \quad (25)$$

538 It seems that this type of behavior is the most natural from the
 539 viewpoint of social connections during the covid-19 epidemic in Swe-
 540 den. Barriers are sufficiently high, but they still are not walls as
 541 during the rigid quarantine (as say in Italy, France, or Russia). For
 542 such linearly increasing barriers one can derive the following asymp-
 543 totic behavior (23) of the relaxation probability [48], where in physics
 544 and biology the parameter

$$q \equiv 1/\alpha = \frac{T \log p}{\Delta}, \quad (26)$$

545 Here the new parameter T has the meaning of temperature. Thus
 546 behavior of distance between valleys of the energy landscape is deter-
 547 mined by the size of the barrier for one-step jump Δ and temperature.
 548 We rewrite formula (19) for transition probability by using these pa-
 549 rameters:

$$p(x|y) = \frac{C_{T,\Delta}}{|x-y|_p^{1+\Delta/(T \ln p)}}. \quad (27)$$

550 In our model, we introduce the notion of *social temperature* T . As
 551 in physics, this parameter calibrates energy, in our case social energy.
 552 The latter represents the degree of social activity, the magnitude of
 553 social actions. Although the notions of social temperature and energy
 554 are not so well established as in physics, they can be useful in socio-
 555 physical modeling (see [67] and references herein, starting with the
 556 works of Freud and Jung). Probability that the virus jumps from the
 557 elementary social cluster y to another cluster x grows with growth
 558 of social temperature. For high T , virus (or its spreader) easily move
 559 between social clusters. If $T \ll 1$, the infection is practically confined
 560 in clusters. If barrier Δ increases for the fixed parameter T , then the
 561 transition probability decreases and vice versa.

562 Starting with expression (27), we obtain the relaxation asymptotic
 563 in the form:

$$p_I(C, t) \sim t^{-\frac{T \log p}{\Delta}}, t \rightarrow \infty. \quad (28)$$

564 Thus, for large t , the average probability to become infected in social
 565 cluster C decreases quicker with increase of social temperature T .
 566 Decrease of the one-step jump barrier Δ implies the same behavior.
 567 We stress that such simple asymptotics with dependence only on one

568 level barrier Δ is a consequence of the linear increase of barriers with
 569 increase of difference between levels of social hierarchy. Immunity
 570 probability $p_{Im}(C, t)$ behaves in the opposite way. It increases quicker
 571 with increase of social temperature and decrease of the social barrier
 572 Δ .

573 The quantity $\ln p$ can be interpreted statistically as entropy of
 574 the process of distribution of infection into p subclusters coupled to
 575 a vertex. Suppose that a virus can spread with equal probability
 576 $q_i = 1/p$ into each of the subclusters $C_{i_0 \dots i_{k-1}, i}$ of the cluster $C_{i_0 \dots i_{k-1}}$.
 577 Entropy of this spreading equals to

$$\mathcal{E} = - \sum_{i=1}^{p-1} q_i \ln q_i = \ln p. \quad (29)$$

578 In terms of spreading entropy asymptotics (??) can be rewritten as

$$p_{Im}(C, t) \sim 1 - t^{-T\mathcal{E}/\Delta}, t \rightarrow \infty. \quad (30)$$

579 Thus, larger spreading entropy of the social cluster tree implies quicker
 580 approaching herd immunity. Our conjecture is that this formula is
 581 valid for more general process of infection spread, with nonuniform
 582 distribution for probabilities q_i .

583 We turn to representation of $\alpha = \alpha_{soc} + \alpha_{preventing}$, its components
 584 correspond to traditional social constraints in population and prevent-
 585 ing measures introduced by authorities. In the same way, we represent
 586 barrier $\Delta = \Delta_{soc} + \Delta_{preventing}$ and obtain the formula:

$$p_{Im}(C, t) \sim 1 - t^{-T\mathcal{E}/(\Delta_{soc} + \Delta_{preventing})}, t \rightarrow \infty. \quad (31)$$

587 Since Δ_{soc} is difficult to change, we shall consider it as constant and
 588 to simplify the model, we set $\Delta_{soc} = 0$. Thus we play just with the
 589 magnitude of the preventing barrier $\Delta_{preventing}$. We also assume that
 590 the social temperature during the epidemic is constant (and relatively
 591 small), again for simplicity we set $T = 1$. Then

$$p_{Im}(C, t) \sim 1 - t^{-\mathcal{E}/\Delta_{preventing}}, t \rightarrow \infty. \quad (32)$$

592 If $\Delta_{preventing}$ is high (rigid anti-epidemic measures of the lock-down
 593 type), then approaching herd immunity is very slow, practically impos-
 594 sible. If $\Delta_{preventing}$ is low, then herd immunity is approached rapidly.

595 Of course, herd immunity is not the only parameter determining
 596 authorities strategy with respect to an epidemic. Much more impor-
 597 tant is the cumulative death rate. However, our model describes only
 598 asymptotic behavior and we cannot calculate cumulative death rates
 599 corresponding to preventing barriers of various magnitudes. We shall
 600 plan to do this in a forthcoming paper.

6 Concluding remarks

In this paper, we continue development of a new mathematical model of disease spread reflecting specialties of covid-19 epidemic (see also []). We especially emphasize the social cluster character of disease spread, **ASO**, for such diseases as covid-19. Clustered spread of say a virus can be modeled with dynamical systems on ultrametric spaces. Social clusters are represented by ultrametric balls. The basic feature of ultrametric balls is that they are either disjoint or one is included in another. This is the root of a the hierarchic structure of an ultrametric space. Geometrically ultrametric spaces are represented by trees with balls given by bunches of branches with the common root.

In this paper, we model the dynamics of coronavirus with ultrametric diffusion equation⁶, its simplest version corresponding to p -adic trees and linearly increasing social barriers. Asymptotic of probability $p_{\text{Im}}(t)$ to become immune against the virus is presented at Fig. 2. Generally, it increases slowly, the speed of increasing depends on the basic parameter of the model $q = T \log p / \Delta$.

In a society with low social temperature and high barriers between social clusters, $p_{\text{Im}}(t)$ increase so slowly that there is practically no hope to approach herd immunity.

Acknowledgments

The author would like to thank Philippe Grangier who stimulated this research by his own attempt to model covid-19 spread (unpublished) and provided interesting information about disease clustering in France as well as for discussion on covid-19 “hidden variables”, Sergey Kozyrev for discussions on ultrametric dynamics, Anja Nertyk information about epidemic in Sweden, and Arkady Plotnisky and Karl Svozil for providing information from American and Austrian sources.

⁶The use of purely diffusional model is supported by specialties of covid-19 epidemic, presented in appendix 1. Of course, this model is only approximate. But, it seems that it gives the right asymptotic of probabilities, to become infected and immune, in socially clustered society.

Appendix 1: Specialties of covid-19 spread supporting our model

As was emphasized in introduction, covid-19 epidemic has some specialties. To match these specialties, one has to develop new mathematical models. The fundamental specialty is the social cluster character of coronavirus spread, see **AS0**. Further, we shall discuss a few other virus' features. They justify the following assumption distinguishing our purely diffusional model of disease spread from the standard SIR-type models:

AS1 *Intensity of virus spreading is relatively insensible to the total number of those who have already been infected.*

Now we discuss a few biological and social factors behind this feature of the virus.

- **Covid on surface.** As was shown in study [62], the probability to become infected through some surface (say in a buses, metro, shop) is practically zero. It was found that even in houses with many infected (symptomatic) people, the viruses on surfaces (of say tables, chairs, mobile phones) were too weak to infect anybody. (Their were present, but were not able to infect mouths.)⁷
- **Covid in air.** The virus is neither so much dangerous at the open air, especially if people follow the recommendation to keep 1, 5 m distance between them. In in [62] was pointed out: “The fact that COVID 19 is a droplet infection and cannot be transmitted through the air had previously also been confirmed by virologist Christian Drosten of Berlin’s Charité. He had pointed out in an interview [63] that coronavirus is extremely sensitive to drying out, so the only way of contracting it is if you were to ‘inhale’ the droplets.”

⁷Mr Streeck, a professor for virology and the director of the Institute of virology and HIV Research at the University Bonn, clarified [62]: “There is no significant risk of catching the disease when you go shopping. Severe outbreaks of the infection were always a result of people being closer together over a longer period of time, for example the apré-ski parties in Ischgl, Austria.” During extended and careful study in Heidelberg (the German epicenter of the covid-19 epidemic) his team could also not find any evidence of living viruses on surfaces. “When we took samples from door handles, phones or toilets it has not been possible to cultivate the virus in the laboratory on the basis of these swabs. ... To actually ‘get’ the virus it would be necessary that someone coughs into their hand, immediately touches a door knob and then straight after that another person grasps the handle and goes on to touches their face.” Streeck therefore believes that there is little chance of transmission through contact with so-called contaminated surfaces.

- 658 • **Asymptomatic individuals.** As was recently announced [64],
659 WOH collected a lot of statistical data showing that asymp-
660 tomatic individuals transmit covid-19 virus to other people with
661 very low probability.⁸ At the same time, US Centers for Disease
662 Control and Prevention estimates that about a third of coro-
663 navirus infections (35%) are asymptomatic [65]. Hence, about
664 35% of infected people practically do not contribute in disease
665 spread.
- 666 • **No mass-events.** Another important restriction supporting
667 **AS1** is that even in Sweden, mass-events were forbidden, so no
668 public concerts, neither football matches.⁹
- 669 • **Superspreaders.** As for many infections, spread of coronavirus
670 has the following feature - the presence of superspreaders of in-
671 fection. One person can infect really many people. Thus, single
672 person’s contribution in disease spread can be essentially higher
673 than contribution of a few hundreds of usual asymptomatic indi-
674 viduals or many presymptomatic individuals (see more on super-
675 spreaders in appendix 2).

676 **AS2** *The number of susceptible people $S(t)$ is so large comparing*
677 *with the number $I(t)$ of those who are infected or the number $R(t)$*
678 *of recovered that we can consider it as constant, $S(t) = \text{const}$, and*
679 *exclude it from model’s dynamical equations.*

680 This assumption implies that for an individual in population under
681 consideration the probability to become infected practically does not
682 depend on the number of recovered. The population is rather far from
683 approaching herd immunity and a disease spreader is surrounded (with
684 the high degree of approximation) by susceptible people. Thus the
685 number of recovered people R also can be excluded from dynamics. Of

⁸“We have a number of reports from countries who are doing very detailed contact tracing. They’re following asymptomatic cases, they’re following contacts and they’re not finding secondary transmission onward. It is very rare – and much of that is not published in the literature,” Van Kerkhove, WOH official said on June 6, 2020. “We are constantly looking at this data and we’re trying to get more information from countries to truly answer this question. It still appears to be rare that an asymptomatic individual actually transmits onward.” [64].

⁹In Sweden, restaurants and night clubs were open, but such events were not of mass-character. The presence in a night club or in a restaurant of one infection spreader has practically the same impact as say 5 spreaders, the effect of closed space. Moreover, the distance between the tables in restaurants also diminished the effect of high number of infected in the population. During the intensive phase of the covid-19 epidemic (the end of March and April 2020) restaurants terminated self-serving during lunches (so typical in Sweden).

686 course, this model provides only the rough picture of the real disease
687 spread, but it reflects the basic features of the covid-19 spread in
688 the states that imposed relatively soft restrictions in relation with
689 epidemic (as, e.g., Sweden, Japan, Belarus).

690 Denote the probability, for a person from social cluster C , to be-
691 come infected at the instance of time t by the symbol $p_I(C, t)$. (We
692 recall that in our ultrametric model social clusters are represented by
693 balls.) Later we shall discuss the interpretation of the notion “prob-
694 ability to become infected” in more detail (section 3). To write the
695 evolution equation for probability $p_I(C, t)$, we impose the additional
696 assumption:

697 **AS3** *The distribution of social clusters in the society is uniform:*
698 *all clusters represented by balls of the same radius have the same mea-*
699 *sure that is equal to balls’ radius.*

700 Mathematically **AS3** is formalized through the use of the Haar
701 measure μ on \mathbf{Q}_p . We understand that this is a strong restriction on the
702 social structure of society. But, the main reason for its imposing is just
703 simplification of mathematics. We can consider other distributions on
704 \mathbf{Q}_p assigning different weights to social clusters represented by balls
705 of the same radius. (We recall that any point of a ball can serve as its
706 center.)

707 Appendix 2: Superspreaders

708 Superspreader is an unusually contagious individual who has been
709 infected with disease; someone who infected the number of people far
710 exceeding the two to three. As was pointed out in MIT Technology
711 Review [66]: “For covid-19, this means 80% of new transmissions are
712 caused by fewer than 20% of the carriers – the vast majority of people
713 infect very few others or none at all, and it is a select minority of
714 individuals who are aggressively spreading the virus. A recent preprint
715 looking at transmission in Hong Kong supports those figures, while
716 another looking at transmission in Shenzhen, China, pegs the numbers
717 closer to 80/10. Lots of outbreaks around the world have been linked
718 to single events where a superspreader likely infected dozens of people.
719 For example, a choir practice in Washington State infected about 52
720 people; a megachurch in Seoul was linked to the majority of initial
721 infections in South Korea; and a wedding in Jordan with about 350
722 guests led to 76 confirmed infections.” The bad news is that, for the
723 moment, we cannot identify diagnostically superspreaders.

Appendix 3: Hidden variables of covid-19 spread

As was discussed in section 3, probability $p_I(C, t)$ is determined by the epidemic context in cluster C at time t , $\mathcal{C}(C, t)$. In principle, this context can be described by hidden variables of epidemiological, social, geographic, economic nature. However, as was already stressed, it is difficult if possible at all to determine these variables for concrete social cluster C and the instant of time t . We illustrate this problem by a number of examples.

For example, covid-19 epidemic in Sweden was characterized by mass spread of infection in nursing homes in Stockholm, but nothing similar happened in other Swedish towns, say in Gothenburg, the second largest city in Sweden. This town is very densely connected with Stockholm with intensive train connection. Trains connection was not restricted during epidemic and (what is more important) during the initial stage of epidemic, in March, people traveled very actively between two towns. Then, theoretically the virus approached Sweden with tourists coming back from skiing in Alps and Stockholm is pointed as the place of arrival, this justifies the mass spread of covid-19 in Stockholm. But, essential part of tourists living in South Sweden (the most densely populated) returned from Alps via the Copenhagen airport (with intensive train communication over the bridge between Denmark and Sweden). However, the virus did not spread in South Sweden, including the third largest city Malmö, neither in Copenhagen. What is the difference between Swedish tourists (coming from the same place in Italian and Austrian Alps) arriving to Stockholm or to Copenhagen? There are hidden variables, but it is difficult if possible at all to determine them. The same can be said about disease spread in nursery homes in Stockholm vs. Gothenburg. Of course, there were attempts to determine “covid-19 hidden variables”; say, for Stockholm’s nursery homes, responsibility for infecting of elderly people was appointed to the personal of these homes. However, there were reported numerous cases in that the personal of nursery homes was widely infected, but the disease did not spread to elderly patients of these homes.

Another interesting fact is about French hospitals: at the beginning, many nurses and doctors got sick, so they were taking extreme precautions. But some (actually most) of them did not get sick, and as time went they all relaxed the precautions, and they still did not get sick, at least not at a noticeable level. Another fact is the gigantic air carrier Charles de Gaulle, with 1700 staff on board, extremely confined. Within a few days more that 60% were tested positive, but

766 actually very few got really sick, only one was seriously ill, and none
767 died. This kind of reaction of the personal of Charles de Gaulle air-
768 port is amazing contrast with reaction of the personal of Stockholm's
769 airport Arlanda, many workers and members of their families were
770 heavily sick.

771 Of course, the most amazing is difference between social clusters
772 determined by nationalities, especially clusters of immigrants. For
773 example, in New York the situation is described as following [68]:

774 "At a clinic in Corona, a working-class neighborhood in Queens,
775 more than 68 percent of people tested positive for antibodies to the
776 new coronavirus. At another clinic in Jackson Heights, Queens, that
777 number was 56 percent. But at a clinic in Cobble Hill, a mostly
778 white and wealthy neighborhood in Brooklyn, only 13 percent of peo-
779 ple tested positive for antibodies. As it has swept through New York,
780 the coronavirus has exposed stark inequalities in nearly every aspect
781 of city life, from who has been most affected to how the health care
782 system cared for those patients. Many lower-income neighborhoods,
783 where Black and Latino residents make up a large part of the popula-
784 tion, were hard hit, while many wealthy neighborhoods suffered much
785 less."

786 Similar picture we can see in Sweden:

787 "New figures in Stockholm confirm the picture that so-called vul-
788 nerable areas are hardest hit by the coronavirus. In the immigrant-
789 rich districts of Rinkeby and Tensta, around 40 people per 10,000 have
790 been infected, which is three times more than the average for the en-
791 tire region. The figures show that the difference with more disease
792 cases in Rinkeby-Kista and Spanga-Tensta has persisted", says Per
793 Follin, infection control doctor in the Stockholm region [69].

794 Generally evolution of such epidemics as covid-19 have to be stud-
795 ied by using information methods similar to paper [70, 71].

796 References

- 797 [1] A. Khrennikov, Ultrametric model for covid-19 dynamics: an
798 attempt to explain slow approaching herd immunity in Swe-
799 den. <https://www.preprints.org/manuscript/202007.0037/v1> ;
800 <https://www.medrxiv.org/content/10.1101/2020.07.04.20146209v1>
801 .
- 802 [2] Khrennikov A., Human subconscious as a p-adic dynamical sys-
803 tem. *Journal of Theoretical Biology*, 193(2), 179-96 (1998).
- 804 [3] S. Albeverio, A. Khrennikov, P. E. Kloeden, Memory retrieval as
805 a p-adic dynamical system. *Biosystems* 49, N 2, 105-115 (1999).

- 806 [4] D. Dubischar, V. M. Gundlach, O. Steinkamp, A. Khrennikov,
807 A p -Adic Model for the Process of Thinking Disturbed by Phys-
808 iological and Information Noise. *Journal of Theoretical Biology*
809 197(4), 451-67 (1999).
- 810 [5] A. Khrennikov, *Information Dynamics in Cognitive, Psycholog-
811 ical, Social, and Anomalous Phenomena*. Kluwer, 2004
- 812 [6] A. Khrennikov, Probabilistic pathway representation of cogni-
813 tive information. *Journal of Theoretical Biology* 231, N 4, 597-
814 613 (2004).
- 815 [7] A. Khrennikov, Toward an adequate mathematical model of
816 mental space: Conscious/unconscious dynamics on m -adic trees.
817 *Biosystems* 90, N 3, 656-675 (2007).
- 818 [8] Murtagh, F. The Haar wavelet transform of a dendrogram. *J.
819 Classif.* 2007, 24, 3–32.
- 820 [9] Dragovich, B.; Dragovich, A. A p -Adic model of DNA sequence
821 and genetic code. *P-Adic Numbers Ultramet. Anal. Appl.* 2009,
822 1, 34–41.
- 823 [10] Dragovich, B.; Dragovich, A. p -adic modelling of the genome
824 and the genetic code. *Comput. J.* 2010, 53, 432–442.
- 825 [11] Murtagh, F.; Contreras, P. Fast, linear time, m -adic hierarchi-
826 cal clustering for search and retrieval using the Baire metric,
827 with linkages to generalized ultrametrics, hashing, formal con-
828 cept analysis, and precision of data measurement. *P-Adic Num-
829 bers Ultramet. Anal. Appl.* 2012, 4, 45–56.
- 830 [12] Contreras, P.; Murtagh, F. Fast, linear time hierarchical clus-
831 tering using the Baire metric. *J. Classif.* 2012, 29, 118–143.
- 832 [13] Vladimirov, V.S.; Volovich, I.V.; Zelenov, E.I. *P-Adic Analysis
833 and Mathematical Physics*; WSP: Singapore, 1994.
- 834 [14] Kochubei, A. N.: *Parabolic Equations over the Field of p -Adic
835 Numbers*, *Math. USSR Izvestiya* 39(1992), 1263-1280
- 836 [15] S. Albeverio and X. Zhao, Measure-valued branching processes
837 associated with random walks on p -adics. *Ann. Probab.* 28,
838 (2000), 1680-1710.
- 839 [16] Kochubei, A.N. *Pseudo-Differential Equations and Stochastics
840 over Non-Archimedean Field*; CRC Press: New York, NY, USA,
841 2001
- 842 [17] V. A. Avetisov, A. H. Bikulov, S. V. Kozyrev and V. A. Osipov,
843 p -adic models of ultrametric diffusion constrained by hierarchi-
844 cal energy landscapes. *J. Phys. A: Math. Gen.* 35, 2002, 177-190.

- 845 [18] Kozyrev, S.V. Ultrametric dynamics as a model of interbasin
846 kinetics. *J. Comput. Math. Anal.* 2006, 41, 38–48.
- 847 [19] Kozyrev, S.V. Ultrametric analysis and interbasin kinetics. *AIP*
848 *Conf. Proc.* 2006, 826, 121–128.
- 849 [20] S. Albeverio, A. Yu Khrennikov, V. M. Shelkovich, *Theory of*
850 *P-adic Distributions: Linear and Nonlinear Models.* Cambridge
851 Univ. Press, Cambridge, 2010.
- 852 [21] Casas-Sanchez, O.F.; Zuniga-Galindo, W.A. P-adic elliptic
853 quadratic forms, parabolic-type pseudodifferential equations
854 with variable coefficients and Markov processes. *P-Adic Num-*
855 *bers Ultramet. Anal. Appl.* 2014, 6, 120–139.
- 856 [22] Volovich, I.V. p-Adic string. *Class. Quantum Gravity* 1987, 4,
857 83–87.
- 858 [23] Dragovich, B.G. Adelic harmonic oscillator. *Int. J. Mod. Phys.*
859 *A* 1995, 10, 2349–2359. [CrossRef]
- 860 [24] Khrennikov, A.Y. *P-Adic Valued Distributions in Mathematical*
861 *Physics;* Kluwer: Dordrecht, The Netherlands, 1994.
- 862 [25] R. M. Anderson, R. M. May, *Infectious Diseases of Humans:*
863 *Dynamics and Control* (Oxford Univ. Press, 1991).
- 864 [26] H. Andersson, T. Britton, *Stochastic Epidemic Models and*
865 *Their Statistical Analysis* (Springer, 2000).
- 866 [27] O. Diekmann, H. Heesterbeek, T. Britton, *Mathematical Tools*
867 *for Understanding Infectious Disease Dynamics* (Princeton
868 Univ. Press, 2013).
- 869 [28] D. Smith and L. Moore, *The SIR Model for Spread*
870 *of Disease - The Differential Equation Model.*
871 [https://www.maa.org/press/periodicals/loci/joma/the-sir-](https://www.maa.org/press/periodicals/loci/joma/the-sir-model-for-spread-of-disease-the-differential-equation-model)
872 [model-for-spread-of-disease-the-differential-equation-model.](https://www.maa.org/press/periodicals/loci/joma/the-sir-model-for-spread-of-disease-the-differential-equation-model)
- 873 [29] K. I. Kim, Zh. Lin, Q. Zhang, An SIR epidemic model with
874 free boundary. *Nonlinear Analysis: Real World Appl.*, 14, 2013,
875 1992-2001.
- 876 [30] S. Flaxman, S. Mishra, A. Gandy, H. J. T. Unwin, H. Coup-
877 land, T. A. Mellan, H. Zhu, T. Berah, J. W. Eaton, P. N. P.
878 Guzman, N. Schmit, L. Cilloni, K. E. C. Ainslie, M. Baguelin,
879 I. Blake, A. Boonyasiri, O. Boyd, L. Cattarino, C. Ciavarella,
880 L. Cooper, Z. Cucunubá, G. Cuomo-Dannenburg, A. Dighe, B.
881 Djaafara, I. Dorigatti, S. van Elsland, R. FitzJohn, H. Fu, K.
882 Gaythorpe, L. Geidelberg, N. Grassly, W. Green, T. Hallett, A.
883 Hamlet, W. Hinsley, B. Jeffrey, D. Jorgensen, E. Knock, D. Lay-
884 don, G. Nedjati-Gilani, P. Nouvellet, K. Parag, I. Siveroni, H.

- 885 Thompson, R. Verity, E. Volz, C. Walters, H. Wang, Y. Wang,
886 O. Watson, P. Winskill, X. Xi, C. Whittaker, P. G. T. Walker, A.
887 Ghani, C. A. Donnelly, S. Riley, L. C. Okell, M. A. C. Vollmer,
888 N. M. Ferguson, S. Bhatt, Report 13: Estimating the number of
889 infections and the impact of non-pharmaceutical interventions
890 on COVID-19 in 11 European countries (Imperial College Lon-
891 don, 2020); .doi:10.25561/77731
- 892 [31] N. M. Ferguson, D. Laydon, G. Nedjati-Gilani, N. Imai, K.
893 Ainslie, M. Baguelin, S. Bhatia, A. Boonyasiri, Z. Cucunubá,
894 G. Cuomo-Dannenburg, A. Dighe, I. Dorigatti, H. Fu, K.
895 Gaythorpe, W. Green, A. Hamlet, W. Hinsley, L. C. Okell, S.
896 van Elsland, H. Thompson, R. Verity, E. Volz, H. Wang, Y.
897 Wang, P. G. T. Walker, C. Walters, P. Winskill, C. Whittaker,
898 C. A. Donnelly, S. Riley, A. C. Ghani, Report 9: Impact of non-
899 pharmaceutical interventions (NPIs) to reduce COVID-19 mor-
900 tality and healthcare demand (Imperial College London, 2020);
901 10.25561/77482.doi
- 902 [32] T. Britton, Basic estimation-prediction techniques for Covid-
903 19, and a prediction for Stockholm. Preprint, April 2020 DOI:
904 10.1101/2020.04.15.20066050
- 905 [33] T. Britton, Basic estimation-prediction techniques
906 for Covid-19, and a prediction for Stockholm.
907 <https://www.medrxiv.org/content/10.1101/2020.04.15.20066050v2>
- 908 [34] T. Britton, P. Trapman, F.G. Ball, The disease-
909 induced herd immunity level for Covid-19 is substan-
910 tially lower than the classical herd immunity level.
911 <https://www.medrxiv.org/content/10.1101/2020.05.06.20093336v2>
- 912 [35] W. Bock, B. Adamik, M. Bawiec, V. Bezborodov, M. Bodych,
913 J. P. Burgard, T. Goetz, T. Krueger, A. Migalska, B. Pab-
914 jan, T. Ozanski, E. Rafajlowicz, W. Rafajlowicz, E. Skubalska-
915 Rafajlowicz, S. Ryfczynska, E. Szczurek, P. Szymanski, Mit-
916 igation and herd immunity strategy for COVID-19 is likely
917 to fail. medRxiv 2020.03.25.20043109 [Preprint]. 5 May 2020;
918 .doi:10.1101/2020.03.25.20043109 Abstract/FREE Full Text-
919 Google Scholar
- 920 [36] H. Salje, C. T. Kiem, N. Lefrancq, N. Courtejoie, P. Bosetti,
921 J. Paireau, A. Andronico, N. Hozé, J. Richet, C.-L. Du-
922 bost, Y. Le Strat, J. Lessler, D. Levy-Bruhl, A. Fontanet, L.
923 Opatowski, P.-Y. Boelle, S. Cauchemez, Estimating the bur-
924 den of SARS-CoV-2 in France. Science 10.1126/science.abc3517
925 (2020). doi:10.1126/science.abc3517

- 926 [37] J. Wallinga, P. Teunis, M. Kretzschmar , Using data on so-
927 cial contacts to estimate age-specific transmission parameters
928 for respiratory-spread infectious agents. *Am. J. Epidemiol.* 164,
929 936–944 (2006).
- 930 [38] R. Pastor-Satorras, A. Vespignani, Epidemic spreading in scale-
931 free networks. *Phys. Rev. Lett.* 86, 3200–3203 (2001).
- 932 [39] M. J. Ferrari, S. Bansal, L. A. Meyers, O. N. Bjørnstad , Net-
933 work frailty and the geometry of herd immunity. *Proc. Biol. Sci.*
934 273, 2743–2748 (2006).
- 935 [40] T. Britton, F. Ball, P. Trapman, A mathematical model reveals
936 the influence of population heterogeneity on herd immunity to
937 SARS-CoV-2. *Science* 23 Jun 2020: eabc6810
- 938 [41] M. Mezard, G. Parisi, N. Sourlas, G. Toulouse, and M. Virasoro,
939 *Phys. Rev. Lett.* 52, 1156 (1984).
- 940 [42] R. G. Palmer, *Adv. Phys.* 31, 66a (1982); G. Parisi, *Phys. Rev.*
941 *Lett.* 50, 1946 (1983).
- 942 [43] A. Ansari, J. Berendzen, S. F. Bowne, H. Frauenfelder, I. E. T.
943 Iben, T. B. Sauke, E. Shyamsunder, and R. D. Young, *Proc.*
944 *Natl. Acad. Sci. USA* 82, 5000 (1985).
- 945 [44] R. G. Palmer, D. L. Stein, E. Abrahams, and P. W. Anderson,
946 *Phys. Rev. Lett.* 53, 958 (1984).
- 947 [45] B. A. Huberman and M. Kerszberg, *J. Phys. A* 18, L331 (1985).
- 948 [46] Parisi, *Phys. Rev. Lett.* 43, 1754 (1979).
- 949 [47] Parisi, G.; Sourlas, N. *p*-Adic numbers and replica symmetry
950 breaking. *Eur. Phys. J. B* 2000, 14, 535–542.
- 951 [48] A. T. Ogielski, Dynamics on Ultrametric Spaces. *Phys. Rev.*
952 *Lett.* 55, 1634-1637.
- 953 [49] Public Health Institute of Sweden, Estimates of the
954 peak-day and the number of infected individuals dur-
955 ing the covid-19 outbreak in the Stockholm region,
956 Sweden February–April 2020 [in Swedish] (2020);
957 [www.folkhalsomyndigheten.se/contentassets/2da059f90b90458d8454a04955d1697f/skattning-
958 peakdag-antal-infekterade-covid-19-utbrottet-stockholms-lan-
959 februari-april-2020.pdf](http://www.folkhalsomyndigheten.se/contentassets/2da059f90b90458d8454a04955d1697f/skattning-peakdag-antal-infekterade-covid-19-utbrottet-stockholms-lan-februari-april-2020.pdf).
- 960 [50] Public Health Institute of Sweden: Antikroppstester avviker
961 fran prognoserna – matematikern “ser tva förklaringar”.
962 <https://www.svt.se/nyheter/inrikes/antikroppstester>
- 963 [51] Public Health Institute of Sweden: Yngre personer har
964 högre andel antikroppar. *Sverige Radion*, June 2, 2020;
965 <https://sverigesradio.se/sida/artikel.aspx?programid=83artikel=7487102>

- 966 [52] Tegnell: “Vi får oroande rapporter om utelivet”. SVT, Ny-
967 heter, 20-04-2020; [https://www.svt.se/nyheter/inrikes/tegnell-](https://www.svt.se/nyheter/inrikes/tegnell-vi-far-oroande-rapporter-om-utelivet)
968 [vi-far-oroande-rapporter-om-utelivet](https://www.svt.se/nyheter/inrikes/tegnell-vi-far-oroande-rapporter-om-utelivet)
- 969 [53] Se hur matematikprofessorn räknar ut när Stockholm uppnår
970 flockimmunitet. SVT Nyheter, 20-04-2020.
- 971 [54] G. Holm, Hoppfulla teorin: Sa när vi flockim-
972 munitet redan i juni. Expressen, 10.05.2020.
973 [https://www.expressen.se/nyheter/coronaviruset/hoppfulla-](https://www.expressen.se/nyheter/coronaviruset/hoppfulla-teorin-sa-nar-vi-flockimmunitet-redan-i-juni/)
974 [teorin-sa-nar-vi-flockimmunitet-redan-i-juni/](https://www.expressen.se/nyheter/coronaviruset/hoppfulla-teorin-sa-nar-vi-flockimmunitet-redan-i-juni/)
- 975 [55] A. Obminska, Det här vet vi om coronaviruset. Ny
976 Teknik, 30-06-2020; [https://www.nyteknik.se/samhalle/det-](https://www.nyteknik.se/samhalle/det-har-vet-vi-om-coronaviruset-6985117)
977 [har-vet-vi-om-coronaviruset-6985117](https://www.nyteknik.se/samhalle/det-har-vet-vi-om-coronaviruset-6985117)
- 978 [56] Public Health Institute of Sweden, 18-06-2020;
979 [https://www.folkhalsomyndigheten.se/nyheter-och-](https://www.folkhalsomyndigheten.se/nyheter-och-press/nyhetsarkiv/2020/juni/forsta-resultaten-om-antikroppar-efter-genomgangen-covid-19-hos-blodgivare/)
980 [press/nyhetsarkiv/2020/juni/forsta-resultaten-om-antikroppar-](https://www.folkhalsomyndigheten.se/nyheter-och-press/nyhetsarkiv/2020/juni/forsta-resultaten-om-antikroppar-efter-genomgangen-covid-19-hos-blodgivare/)
981 [efter-genomgangen-covid-19-hos-blodgivare/](https://www.folkhalsomyndigheten.se/nyheter-och-press/nyhetsarkiv/2020/juni/forsta-resultaten-om-antikroppar-efter-genomgangen-covid-19-hos-blodgivare/)
- 982 [57] L. A. Demetrius, V. M. Gundlach, Directionality Theory and
983 the Entropic Principle of Natural Selection. *Entropy* 2014, 16,
984 5428-5522.
- 985 [58] Asano, M., Khrennikov, A., Ohya, M., Tanaka, Y. and Yam-
986 ato, I. (2015). *Quantum adaptivity in biology: from genetics to*
987 *cognition*, Springer: Heidelberg-Berlin-New York.
- 988 [59] Khrennikov, A. (2010). *Ubiquitous quantum structure: from psy-*
989 *chology to finances*; Springer: Berlin-Heidelberg-New York.
- 990 [60] Busemeyer, J. R. and Bruza, P. D. (2012). *Quantum models of*
991 *cognition and decision*, Cambridge University Press, Cambridge.
- 992 [61] Fuchs, C. A., Mermin, N. D. and Schack, R. (2014). An In-
993 troduction to QBism with an Application to the Locality of
994 Quantum Mechanics, *Am. J. Phys.* **82**, p. 749.
- 995 [62] H. Streeck, So far, no transmission of the virus
996 in supermarkets, restaurants or hairdressers has
997 been proved. [https://today.rtl.lu/news/science-and-](https://today.rtl.lu/news/science-and-environment/a/1498185.html)
998 [environment/a/1498185.html](https://today.rtl.lu/news/science-and-environment/a/1498185.html), 14.04.2020.
- 999 [63] Podcast “Coronavirus-Update” mit Christian Drosten.
1000 [https://www.ndr.de/nachrichten/info/14-Coronavirus-Update-](https://www.ndr.de/nachrichten/info/14-Coronavirus-Update-Vorsicht-vor-Vereinfachungen,podcastcoronavirus132.html)
1001 [Vorsicht-vor-Vereinfachungen,podcastcoronavirus132.html](https://www.ndr.de/nachrichten/info/14-Coronavirus-Update-Vorsicht-vor-Vereinfachungen,podcastcoronavirus132.html)
- 1002 [64] J. Howard, Coronavirus spread by asymptomatic peo-
1003 ple appears to be rare,“ WHO official says. CNN,
1004 [https://edition.cnn.com/2020/06/08/health/coronavirus-](https://edition.cnn.com/2020/06/08/health/coronavirus-asymptomatic-spread-who-bn/index.html)
1005 [asymptomatic-spread-who-bn/index.html](https://edition.cnn.com/2020/06/08/health/coronavirus-asymptomatic-spread-who-bn/index.html)

- 1006 [65] A. Azad, CDC estimates that 35% of coronavirus pa-
1007 tients don't have symptoms. CNN, May 22, 2020,
1008 [https://edition.cnn.com/2020/05/22/health/cdc-coronavirus-](https://edition.cnn.com/2020/05/22/health/cdc-coronavirus-estimates-symptoms-deaths/index.html)
1009 [estimates-symptoms-deaths/index.html](https://edition.cnn.com/2020/05/22/health/cdc-coronavirus-estimates-symptoms-deaths/index.html)
- 1010 [66] Technology Review, What's a coronavirus superspreader?
1011 [https://www.technologyreview.com/2020/06/15/1003576/whats-](https://www.technologyreview.com/2020/06/15/1003576/whats-a-coronavirus-superspreader/)
1012 [a-coronavirus-superspreader/](https://www.technologyreview.com/2020/06/15/1003576/whats-a-coronavirus-superspreader/) 15.06.2020.
- 1013 [67] A. Khrennikov, Social Laser. Jenny Stanford Publ., Singapore,
1014 2020.
- 1015 [68] J. Goldstein, 68% Have antibodies in this
1016 clinic. Can a neighborhood beat a next wave?
1017 [https://www.nytimes.com/2020/07/09/nyregion/nyc-](https://www.nytimes.com/2020/07/09/nyregion/nyc-coronavirus-antibodies.html)
1018 [coronavirus-antibodies.html](https://www.nytimes.com/2020/07/09/nyregion/nyc-coronavirus-antibodies.html) ; 9.07.2020.
- 1019 [69] I. Garcia, Omradena som drabbats hardast av corona i Stock-
1020 holm.
1021 <https://sverigesradio.se/sida/artikel.aspx?programid=83&artikel=7447621>
1022 ; 7.04.2020.
- 1023 [70] K Sato and M. Ohya, Evolution of HIV-1 from the viewpoint of
1024 information theory. 2010 3rd International Symposium on Ap-
1025 plied Sciences in Biomedical and Communication Technologies
1026 (ISABEL 2010).
- 1027 [71] M. Regoli, From Cryptography to Biology and Vice Versa. Open
1028 Systems and Information Dynamics 18, No. 01, 87-105 (2011).